UNIVERSITY OF PADUA
DEPARTMENT OF PHYSICS AND ASTRONOMY

Heart Rate Estimation

Laboratory of Computational Physics

Andrea Nicolai
Camilla Quaglia
Sandeep Kumar Shekhar
Walter Zigliotto

Abstract

The age of technology has made devices smarter and more robust. The estimation of the heart-beat rate and its implications in the medical industry is becoming trivial. Even though the existing methods give a satisfactory understanding of heart action, there is always room for improvement. The Electrocardiography (ECG) is the most typically used technique, but we make use the concept of Seismocardiography (SCG) to analyse the heart-beat rate, respiratory rate. The sensor used in this technique is robust and the data is analysed using simple algorithms, and well known filtering techniques.

Key words: Heart beat rate, ECG, SCG, Respiratory rate, Algorithms, Filtering techniques.

CONTENTS

1 INTRODUCTION

The modern-day medical equipment requires sophisticated instruments to diagnose and understand any kind of ailments. One of the most studied organs of the body is the heart. The basic instrument used by a practitioner to study the heart is the Stethoscope. The traditional in-depth analysis is an Electrocardiography (ECG) [1]. ECG is a technique that measures the electrical signals of the heart. But there have been other techniques to measure the heartbeat. One of them is Seismocardiography (SCG). The SCG was first introduced to clinical medicine by J. Zanetti (earthquake seismologist) and D. Salerno (cardiologist) in 1987 [2]. SCG effectively picks up the vibrations from the chest, generated by the pumping action of the heart. The major distinctive advantage the SCG has over ECG is that it simultaneously measures Heart Rate (HR) as well as the Respiratory Rate (RR). The sensor is placed on the sternum, and the readings are based on the accelerometer and gyroscope or the combination of both. An accelerometer is a sensor able to detect the displacement of small mass suspended through an elastic element under the effect of a force. Gyroscope is another sensor placed along with the accelerometer, which measures the angular velocity under the effect of the Coriolis force. Another technique similar to that of SCG is the Ballistocardiography (BCG). It is a method to obtain HR and the RR without the sensor being in contact with the body [3]. The dawn of the age of electronics has enhanced the performance of the sensor, on which the SCG and the BCG techniques solely rely on. The combination of these techniques along with the ECG aids us to understand the electrochemical and electro-mechanical performance of the heart. This work involves the analysis of data obtained from the sensor, placed on two different subjects. The sensor was once placed on the sternum and another time under the mattress. A similar data analysis technique is used on both occasions.

2 SENSOR PLACED ON THE STERNUM

2.1 DATA PREPARATION

The data obtained from the sensor placed on the sternum is imported as a 'txt' file. The file contains the measurements of the accelerometer and the gyroscope, out of which 7 columns are of significance for our studies. The data acquisition rate is $200\,Hz$, and the columns related to the acceleration and gyroscopic movements in X, Y and Z directions are selected. From the acquisition frequency, we know that the sampling interval is constant, from which the time is extracted. Alongside the accelerometer and gyroscopic measurements, the original file consists of the mode of acquisition, the sampling frequency and the quarternions.

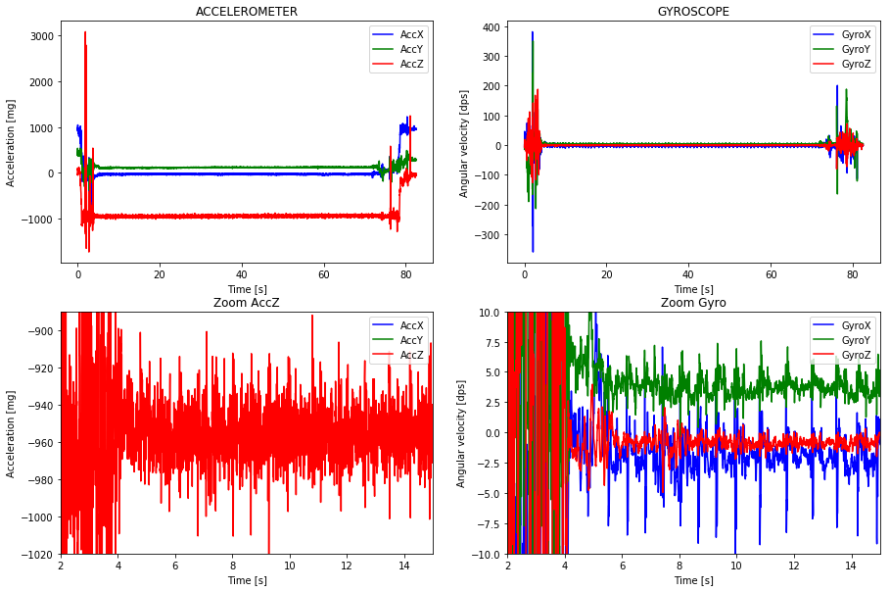

Figure 2.1: The accelerometer and the gyroscope measurements in X, Y, Z directions are plotted against time. The magnified versions of the acceleration in Z axis and the gyroscope in all the axes.

From the plot seen above (as in fig. 2.1), we have selected a suitable time window, in order to omit the extremes of the time interval. This is done to extract only the information of relevance and to remove the noise. The noise is probably because of the positioning of the sensor on the body. The careful selection of the time window reduces the data set to the dimension of 12000 X 7.

2.2 STATISTICAL DESCRIPTION OF THE DATA SET

The table shown below (fig. 2.2) is useful to understand the variation in the values, which serves as a useful tool for further analysis of the data. The key thing to be noted is the mean of the accelerometer measurement in the Z axis is close to the acceleration due to gravity of

the earth ($g = 9.81 m/s^2$). This is due to the placement of the sensor on the sternum, which is oriented in the direction of the Z axis. Another highlight from the table is the standard deviation of the Z axis of the accelerometer that is really high when compared to the other axis. This gives us an unequivocal precedence to choose the Z axis for further analysis. The standard deviation of the mean is given as:

$$\sigma_{mean} = \frac{\sigma}{\sqrt{N}} \tag{2.1}$$

	AccX [mg]	AccY [mg]	AccZ [mg]	GyroX [rad/s]	GyroY [rad/s]	GyroZ [rad/s]
count	12000.0	12000.0	12000.0	12000.0	12000.0	12000.0
mean	-30.7	115.6	-949.1	-2.1	3.7	-0.9
std	7.0	5.3	14.4	1.4	0.7	0.4
min	-66.9	85.8	-1015.5	-10.0	0.5	-2.5
25%	-35.3	112.1	-957.6	-2.7	3.3	-1.1
50%	-30.6	115.7	-949.5	-2.2	3.6	-0.9
75%	-26.0	119.1	-941.3	-1.5	4.0	-0.6
max	-5.4	147.4	-879.7	4.5	7.6	0.6

Figure 2.2: The table depicting the statistical information of the chosen data set.

Where σ is the standard deviation given in the table and the N is the number of the samples (12000). Since we have a large data set the mean is good descriptor for analysis. The percentiles are not of significance for us because, the probability distribution function (PDF) does not concern the analysis.

2.3 Fourier transform analysis of the Accelerometer

2.3.1 Pre-processing

The raw data figure (fig. 2.1) does not provide sufficient details about the heart beat. It consists of required signal and noise, therefore a suitable processing technique is required to extract the signal. The signal has a lot of peaks in a particular section of the time window, like a series of clumps. But one needs to extract the maxima. A fourier analysis helps us to decompose the signal and is essential in finding the maxima. Fast Fourier Transform (FFT) computes the discrete fourier signal (fig. 2.3). From the fig. 2.3, one can find several peaks clumping together in a certain time interval. The selection of the time interval in which the maximum and minimum peak found is required for further analysis.

A Power Spectral Density (PSD) analysis is required to find the time window at which the maxima lies. Basically, PSD uses the concept of weighted mean or moving mean to define a spectrum of peaks on a fourier analysis (fig. 2.3).

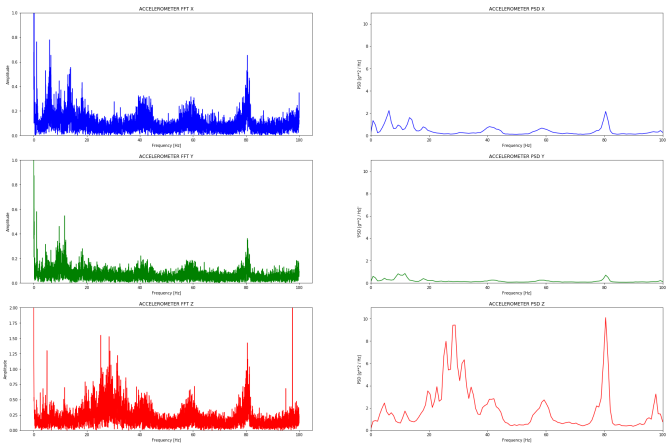

Figure 2.3: Both raw and filtered data clearly shows a pattern with many peaks.

2.3.2 FILTERING

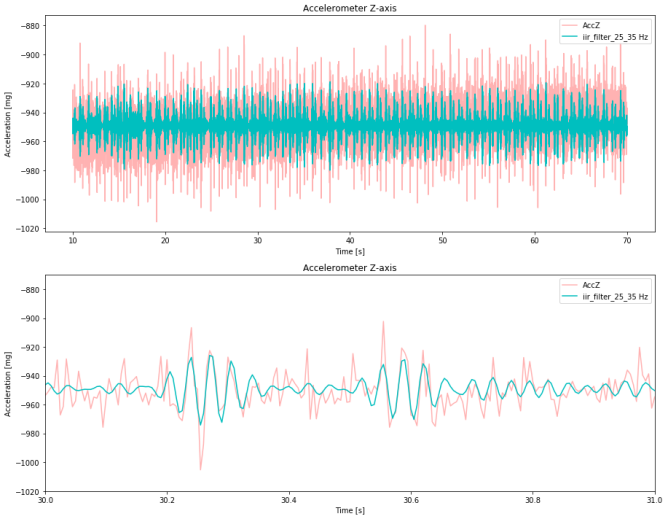

Figure 2.4: The result is filtered in the frequency range of $25-35Hz$.

Once the fourier analysis is done, we need to find a suitable filter to extract a single wave packet for future analysis. An Infinite Input Response (IIR) filter is used. The IIR filter is more like a pass-band filter but it has a selection bandwidth window like an increasing exponential and a decreasing exponential function. The impulse response of the filter does not become 'zero' even after a certain time duration. The bandwidth of $25-35Hz$ is selected because, the opening and closing of the mitral and the aortic valves of the heart lie in this frequency range (fig. 2.4).

It is affirmative to recognize a pattern in our filtered data, our aim is to find the center of a single wave packet that periodically shows up. We can distinguish two of them, that are

related anatomically to two specific events belonging to a single heartbeat (fig. 2.4). The first heart beat generated is due to action of closing of the mitral valve of the heart, vaguely it is the 'lub' sound of the heart [4]. In order to highlight the center, we use the method of convolution of the filtered signal with itself, using a specific transform called 'Hilbert Transform' to obtain the amplitude of the wave train in function of time. The envelope function is used to trace the extremes of the signal and a boolean function is used to detect the maxima of the enveloped signal. As a consequence we try to implement an algorithm in order to compute the time-distance between two large and two small peaks respectively. An assumption is that they belong to different heartbeats. The primitive step is to individuate our local maxima. First, we re-scale and normalize our data to the maximum and minimum amplitude of our dataset, because we are interested only in variations in time, making the computation less cumbersome. In order to neglect peaks that are local maxima, but smaller than the biggest two that is of our interest, a threshold is set as shown in the fig. 2.5.

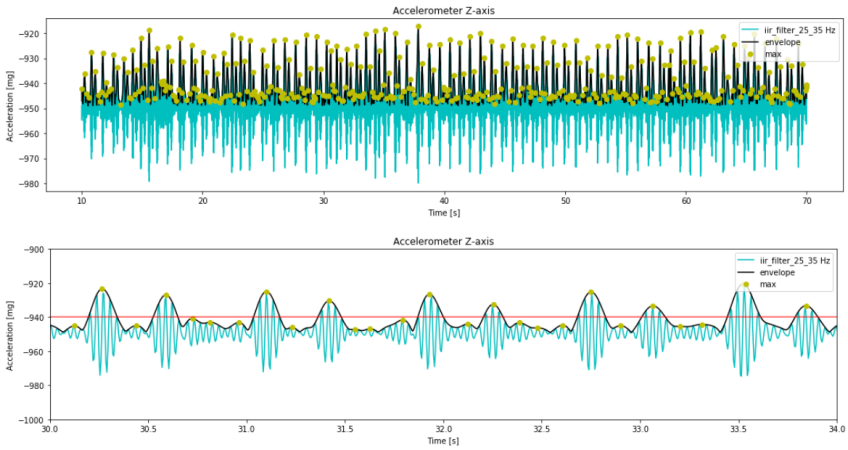

Figure 2.5: The envelope traced to find the maximum of the filtered data.

2.3.3 THE ALGORITHM

Now, we need to find every couple (t_i, A_i) corresponding to the center of a single wave train. In order to do this, we have written a function that returns as a result all points shown below (fig. 2.6), which are both local maxima and above a certain threshold.

Once all the existing local maxima satisfying to our constraints have been figured out, next step is to label peaks according to their nature, either large or small. Since we know a small peak must be both followed and fore-run by a larger one, and holding vice-versa, we can tell the nature of a single peak by simply analyzing whether its neighbours are both smaller or larger than itself (graphically shown in fig. 2.7). In that case, a different label is used according to the type of the peak being a large or a small one. It may happen that a local maximum is not followed and preceded by a pair of peaks of the same kind, in that case an undefined label is assigned to it. This might occur, for example, when the small peak is below the threshold

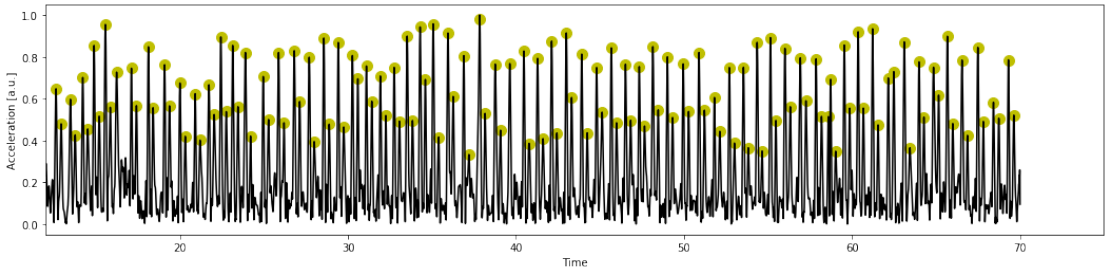

Figure 2.6: Results of function returning all maxima of our data set.

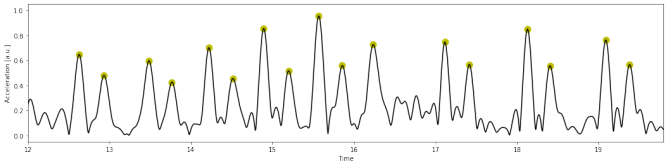

Figure 2.7: fig. 2.6 has been magnified in [12:20]s region.

we have set, thus not detecting it. fig. 2.8 shows the color coding for the differentiation of the peaks according to the above idea. fig. 2.9 gives a magnified version of fig .2.8 in a certain time window.

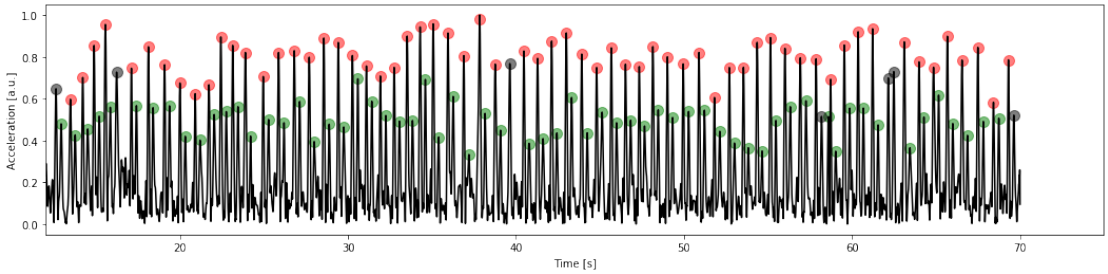

Figure 2.8: Result of the intermediate step of the algorithm, green dots are small peaks, while red are large ones. Black dots are indeed undefined.

We now proceed to compute time-distances between large-large peaks and small-small peaks: since they belong to different heartbeats and moreover they are periodic, we can thus estimate the duration of heartbeat from two different sub-samples and finally analyze the results. In order to compute the time distance between two peaks, keeping in mind the constraint we have fixed about having the same label, we iterate along all peaks that have been already found before. Having chosen one, we see whether the one before and the one after are of the same nature. If so, then the distance is computed.

Results for these intermediate steps are $0.86s \pm 0.08s$ for time distances between two large peaks, and $0.85s \pm 0.10s$ for times distances between two small peaks.

Since some maxima are labeled as undefined because the previous or the following nature

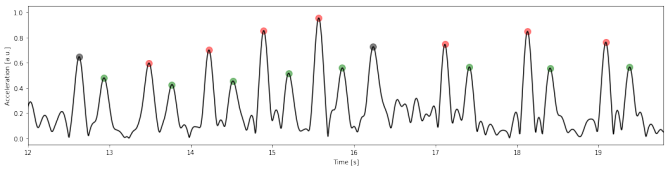

Figure 2.9: fig.2.8 has been magnified in [12:20]s region.

of the peak is unknown, we can assume that the following related peak follows an exponential distribution centered in the estimate as obtained before. fig. 2.10 gives the described distribution.

$$pdf(x|\mu) = \frac{1}{\lambda} \exp^{-\lambda|x-\mu|} \tag{2.2}$$

Where μ is our offset to center our distribution in the estimate we computed before, and λ is the mean obtained in the previous estimates.

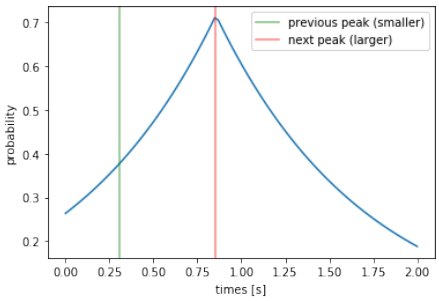

Figure 2.10: Exponential distribution centered in our HB duration estimate, used to weight peaks, being the starting peak in zero (a large one).

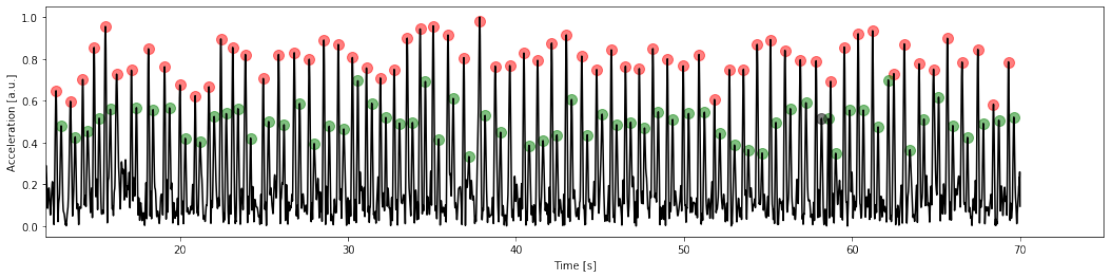

Figure 2.11: Final result of first step of the algorithm.

We now assume that the time between a heartbeat and successive one distributes regardless of the past ones, so our process is said to be 'memory-less'. This can be a reasonable estimate for a healthy person (no diseases related to HRV), resting while the data acquisition is running. We use this assumption to weight peaks that were previously labeled as undefined

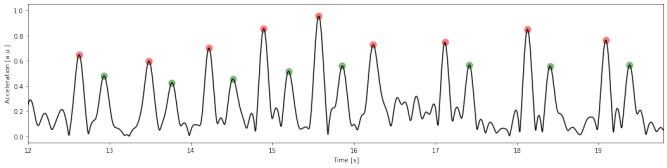

Figure 2.12: fig. 2.11 has been magnified in [12:20]s region.

ones. Starting from a single undefined point we compute time distance between itself along with its predeceasing and the successive point. Then, we notice the probability to have a peak at a given heart rate μ, as obtained previously for the two different times. Labeling the peak accordingly to the largest probability only if it is above a certain confidence threshold, which was set to 0.5. Otherwise, it would remain undefined. Running this last step of our algorithm, we could manage to label some peaks that previously looked like small or large ones, but it was not possible to define them with a good certainty.

We notice as a peak is still undefined, as well as there could be some declassification around 60 seconds, but because of the check implemented in the time-distance computation, the second one in particular is not taken into account. In any case we see for example: that some points have been correctly classified, among these are the very first and the very last one (fig. 2.11, fig. 2.12).

2.3.4 BPM ESTIMATION

Once the labeling of maxima is complete, we now compute the time between a couple of large and a couple of small peaks (fig. 2.13), thus estimating a duration of a heartbeat. This is done by assigning the weighted mean for the two results as done before, because of the optimal compatibility between the values. The compatibility is given as:

$$compatibility = \frac{|\mu_1 - \mu_2|}{\sqrt{\sigma_1^2 + \sigma_2^2}} \tag{2.3}$$

Where μ_1 and μ_2 are the mean of the first and the second principal components respectively. σs represent the standard deviation.

Our μ and σ are $0.85s \pm 0.10s$ for the first histogram related to small peaks, and 0.86 ± 0.08 for the second that is related to large peaks. Since compatibility between the two estimates is really high, we thus proceed to compute a weighted average that returns: $0.85s \pm 0.06s$.

2.3.5 *HRV*: HEART RATE VARIABILITY

In order to diagnose heart diseases such as arrhythmia, technically one needs to look into the duration of a heartbeat, similar to what we dealt in the previous section. We expect it to be as clustered as possible, being very close to the bisector line (fig. 2.14).

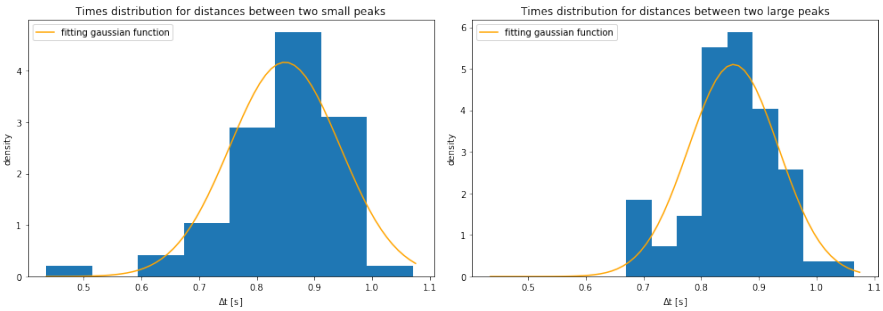

Figure 2.13: Results obtained by running our definitive algorithm.

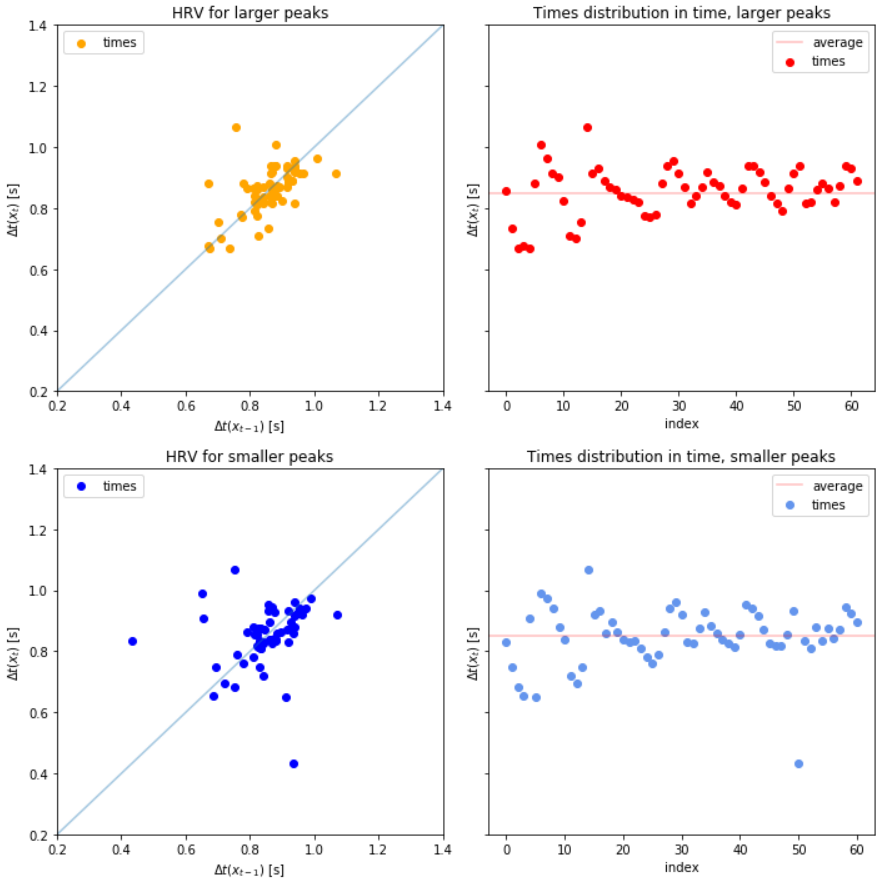

Figure 2.14: HRV on two different subsamples

From this data we can notice only a few points that are spread out (fig. 2.14), especially the ones referring to times computed between two smaller peaks which actually could be mislabelled. Since they are not so many of the mislabelled peaks, it is not a worrisome thing and not to diagnose of the test subject with any disease. Another estimate of the HRV could

be done through the variance (or alternatively the $FWMH$) of the times distributions found previously. Since $\sigma \approx 0.08s$ for both curves is not a large number compared to a heartbeat duration, we obtain results compatible with the plot above at a first sight.

2.4 PCA (Principal Component Analysis)

The statistical distribution obtained gives us the notion of the prominence of accelerometer data in a preferential direction but not for the gyroscope. In order to determine a direction in which the gyroscope measurement is prominent, PCA becomes handy. PCA is a technique which helps us to reduce the dimension, thereby determining the direction by considering the maxima variance in the data and projecting them to a new subspace with less dimensions than the original one. From the chosen data set, for each column such as 'GyroX GyroY GyroZ' the average is calculated. Then the average is subtracted from each element of corresponding column. The definition of the covariance matrix (2 variables):

$$Cov(X,Y) = \frac{\sum_{i=1}^{n}(X_i - \bar{X})(Y_i - \bar{Y})}{n-1} \tag{2.4}$$

From the covariance matrix the eigen values and vectors are computed. Considering the first two main components, related to eigenvalues whose modulus is the largest one, we can explain 96% of the total variability of the system. Thus using them, and projecting the dataframe into the subspace generated by those eigenvectors. In this way we obtain the first two main components, that has been used for our further analysis.

2.5 Frequency analysis of the Gyroscope

By performing the frequency analysis as previously done, we have chosen a frequency band to design the filter for the following analysis. The frequency band of the filter is $0.8-1.5Hz$ as seen in the figure below (fig. 2.15. fig. 2.16 projects a clear distinction between the raw and the filtered data.

2.5.1 The first principal component

fig. 2.17 clearly shows the maxima after the band pass filter processing in the initially described bandwidth. The time interval between the maxima is computed and a histogram plot is obtained (fig. 2.18).

The histogram is fitted with Gaussian distribution. The mean (μ) and the standard deviation (σ) are obtained. These parameters give the first estimation of the heart rate. For this probability distribution the skewness and the kurtosis are estimated. The values for skewness and kurtosis are ≈ 0.1 and ≈ 4.6 respectively. These values of distribution indicates that the distribution is centered around its mean. The expected kurtosis value for a normal distribution is 3, but we find is to be close to 4. This discrepancy is maybe due to number of samples

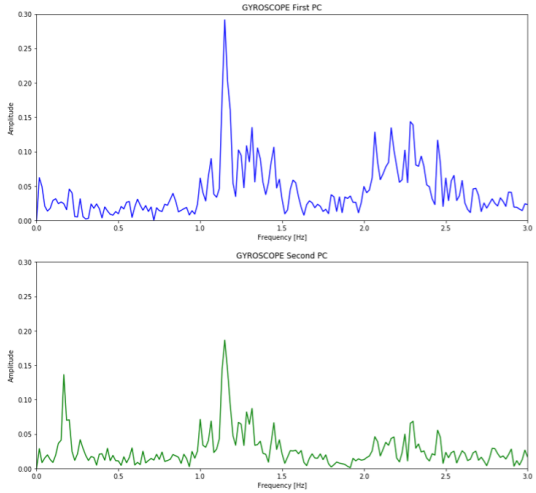

Figure 2.15: The first principal component is shown by the blue color, and the green one denotes the second principal component.

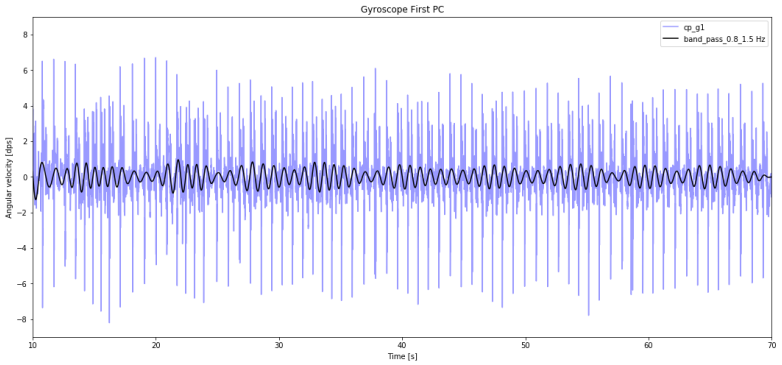

Figure 2.16: The raw data is colored blue and the filtered data is colored black.

used data set are less, when compared to the typical samples used for a normal distribution. Our distribution tends to a leptokurtic distribution.

2.5.2 THE SECOND PRINCIPAL COMPONENT

The second principal component analysis follows a similar pattern and distribution as that of the first principal component and the plots are shown in the fig. 2.19, 2.20, 2.21.

The skewness and the kurtosis are ≈ 0.02 and ≈ 3 respectively. Here, one can notice the value of kurtosis to very close to a kurtosis of a typical normal distribution.

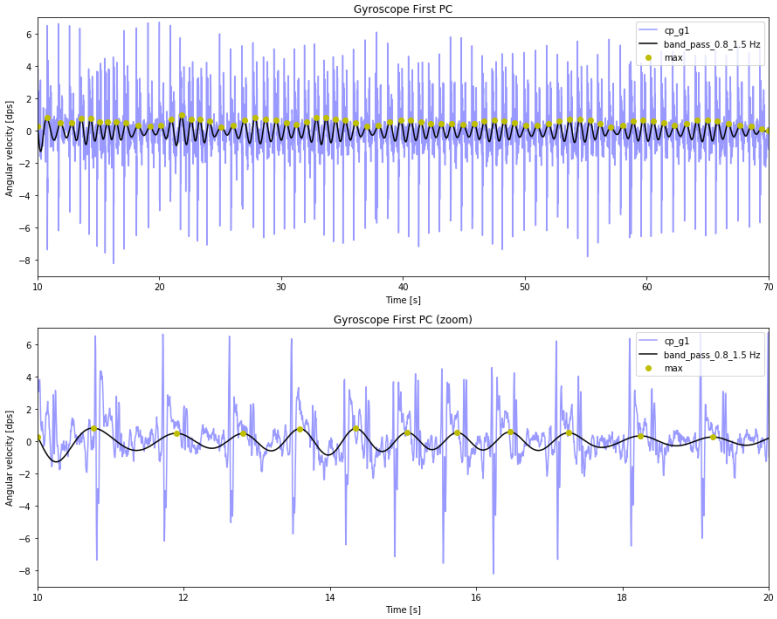

Figure 2.17: Maxima found in the filtered data from the gyroscope first PC.

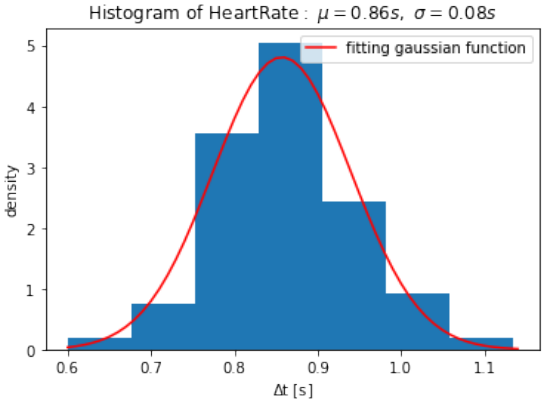

Figure 2.18: The histogram generated for the time intervals.

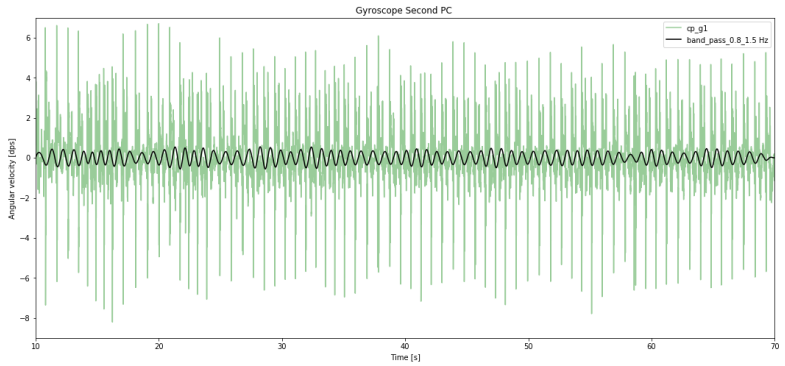

Figure 2.19: The raw data is colored green and the filtered data is colored black.

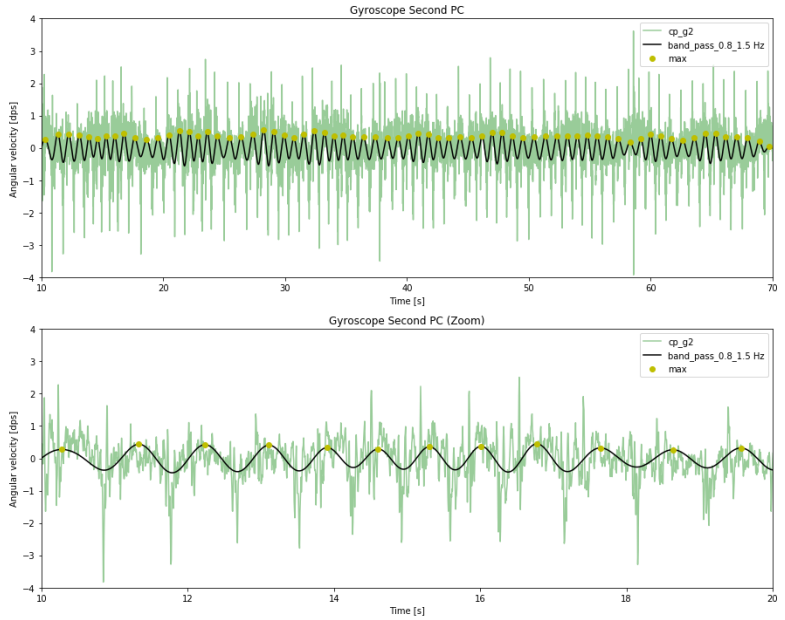

Figure 2.20: Maxima found in the filtered data from the gyroscope second PC.

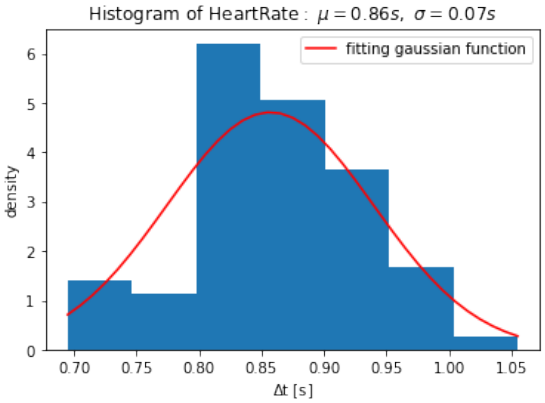

Figure 2.21: The histogram generated for the time intervals.

2.5.3 COMPATIBILITY, *HRV*

This section mainly brings about the relationship between the principal components. For this, the compatibility is given in equation. 2.3.

The calculated result is 0.04. This result suggests a good compatibility. The final HRV estimation is computed by weighted mean and the results are $\mu_{final} \approx 0.86$ and $\sigma_{final} \approx 0.06$.

3 SENSOR PLACED UNDER THE MATTRESS

The sensor placed on the sternum is the most trivial and the most obvious position for one to do measurements. But what if we are put under a constraint of placing elsewhere apart from the body, so that the test subject is not disturbed. One of the optimal place is under the mattress, and above a bed stave. The con of using this procedure is the data from gyroscope will not be able to be analyzed since the sensor is kept fixed and can't rotate.

This translates to the fact that we can use only data provided by the accelerometer sensor along Z axis. But the data from the accelerometer contains more noise, because the sensor is placed under the mattress.

3.1 DATA PREPARATION

The data obtained is in the form of a 'txt' file. The file has similar measurements as said in the section. 2.1. The only difference is the data acquisition rate, which is $100Hz$, and the time window of $60s$ is selected (fig. 3.1). The data acquisition rate is much lower than before because, if we consider higher frequencies the noise gets crept into the signal.

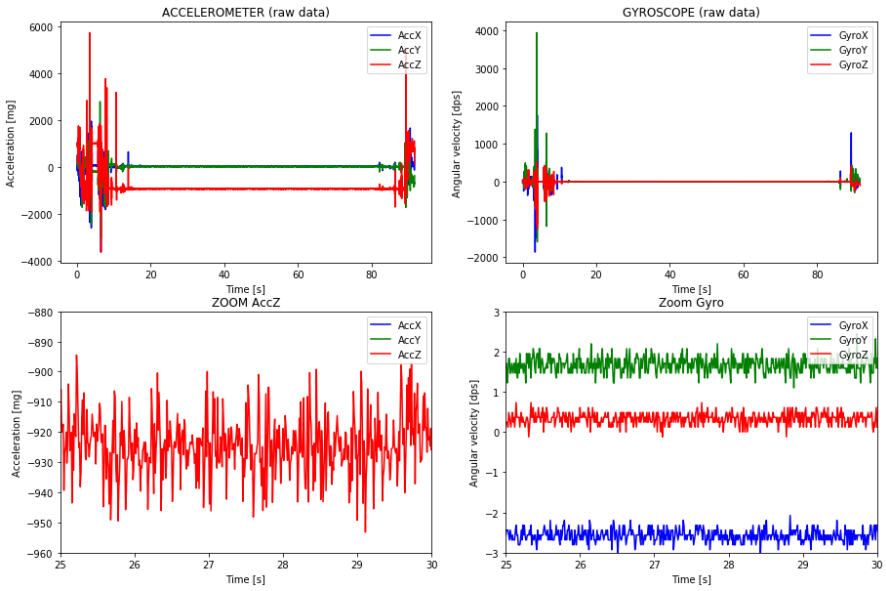

Figure 3.1: The accelerometer and the gyroscope measurements in X, Y, Z directions are plotted against time. The magnified versions of the acceleration in Z axis and the gyroscope in all the axes.

3.2 Statistical Description of the Data Set

As we have done before for the previous data set (fig. 3.2, we observe similar importance of the Z axis and the gyroscope data is of no use because the resolution is proximal to the sensor resolution.

	AccX [mg]	AccY [mg]	AccZ [mg]	GyroX [rad/s]	GyroY [rad/s]	GyroZ [rad/s]
count	6000.0	6000.0	6000.0	6000.0	6000.0	6000.0
mean	44.2	21.5	-924.2	-2.5	1.7	0.3
std	4.6	3.0	9.7	0.1	0.2	0.2
min	26.5	8.3	-954.6	-3.2	1.1	-0.2
25%	41.4	19.6	-929.2	-2.7	1.6	0.2
50%	44.2	21.5	-924.2	-2.6	1.7	0.4
75%	46.9	23.5	-919.1	-2.4	1.8	0.5
max	63.6	33.7	-891.6	-2.1	2.4	1.0

Figure 3.2: The table depicting the statistical information of the chosen data set.

3.3 Fourier Transform Analysis of the Accelerometer

3.3.1 Pre-processing

The statistical description shows us the importance of Z axis, henceforth the processing and filtering will be done only on the Z axis. The similar FFT and PSD analysis is done and the plot is obtained below in fig. 3.3.

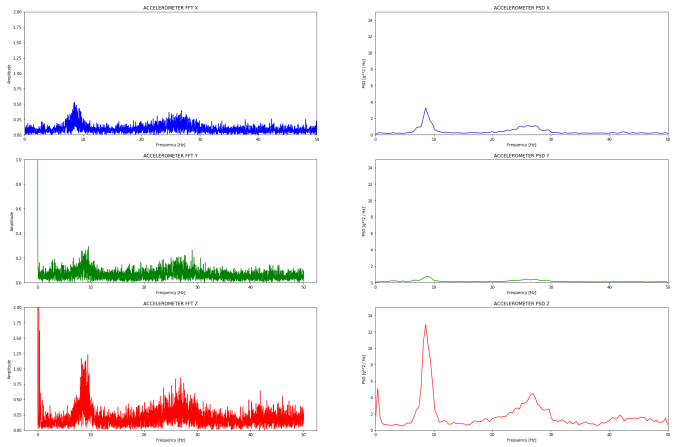

Figure 3.3: Both raw and filtered data clearly shows a pattern with two peaks.

3.3.2 FILTERING

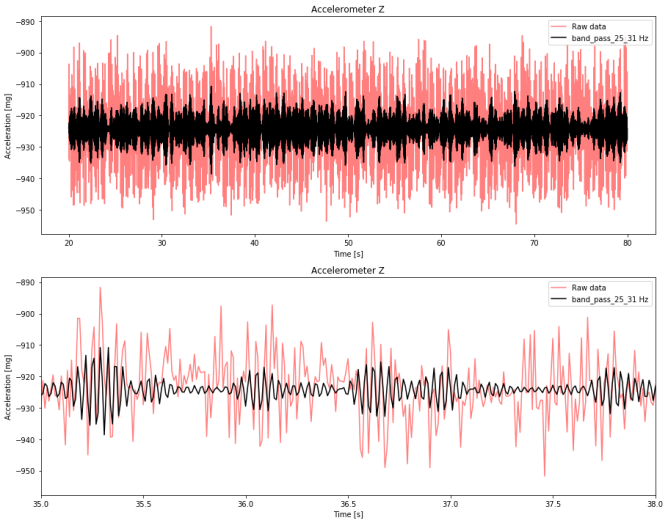

Figure 3.4: The result is filtered in the frequency range of $25-31Hz$.

When compared to the previous filtering technique, we use butter-worth filter instead of a IIR filter. Since we do not observe so many peaks in a small time interval clumped together, we do not require the IIR filter. The frequency range for extracting the signal is around $25-31Hz$. This frequency range noted here coincides with the frequency range $(25-35Hz)$ from the data set before. Henceforth making the signal a legit heart beat signal (fig. 3.4). The same kind of envelope procedure as done before is used to determine the maxima as shown in the fig. 3.5.

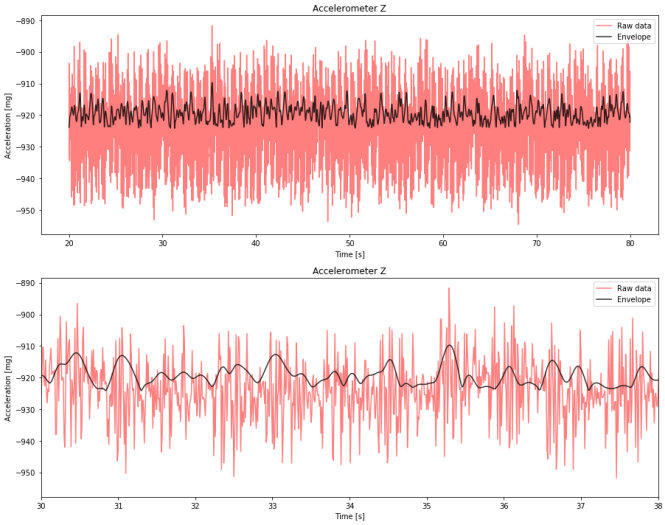

Figure 3.5: The envelope traced to find the maximum of the filtered data.

Once the signal has been given an envelope, filters are reused once more to obtain the required maxima. The enveloped signal is introduced to a high pass and a low pass filter. The high pass filter gives a signal of many number of peaks clumped together in a short time interval. Whereas a low pass filter gives a much better signal to obtain the maxima (fig. 3.6). This is due to the fact at lower frequencies we have a better resolution between the peaks, therefore aiding in extracting the peaks.

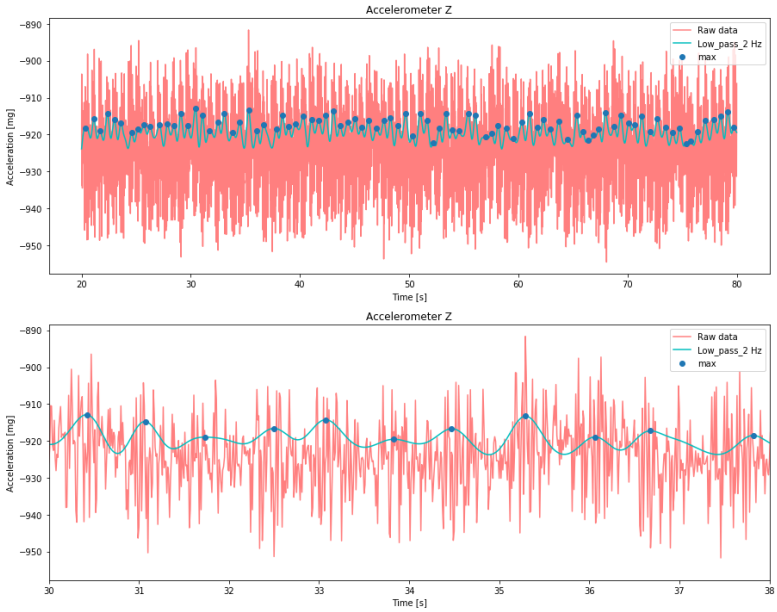

Figure 3.6: The low frequency filter used on the enveloped signal.

A histogram plot is required to observe the distribution of the time intervals between the two successive beat. The gaussian distribution does not fit the data, because the skewness is close to 1 (fig. 3.7). This might be due to the lesser number of samples considered. So we decide to use the statistical mean, the result is $0.7 \pm 0.1s$.

The HRV understanding is important to further correlate with the HRV analysis done for the previous data set. The fig. 2.14 and the figure above (fig. 3.7) show similar variations in the maximum peak estimation, once more confirming the genuinity of the signal.

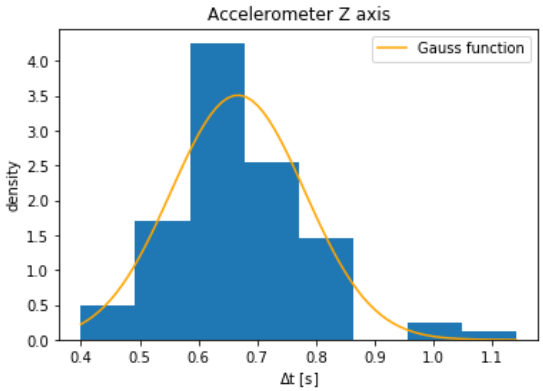

Figure 3.7: A histogram plot to obtain the distribution mean.

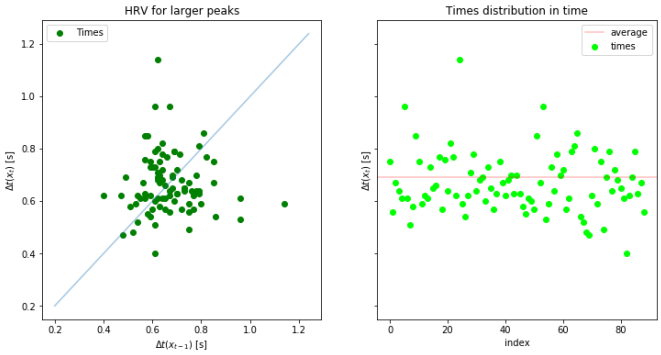

Figure 3.8: HRV for larger peak.

The accuracy of the result plays a prominent role in diagnosing the patient with any kind of heart related issue. Therefore, a better, sophisticated algorithm is needed. The second algorithm makes use of a band pass filter of bandwidth $(1-20)Hz$. A peak can be seen in PSD plot in the $1-20Hz$ range (fig. 3.3), and an Hilbert transform afterward. The importance of the algorithm is to compare with the previous estimates of the heartbeat and compare the accuracy of results with the sensor placed on the sternum. The primitive step is to re-scale our filtered data to its minimum-maximum, as done in the dataset provided by the sensor positioned on the sternum.

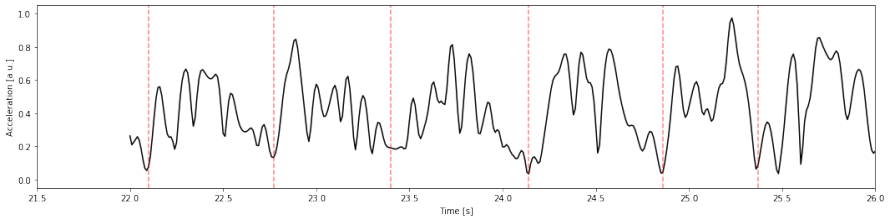

Figure 3.9: Visible pattern and possible period indicated by a red dash line.

A periodic pattern appears from the figure above (fig. 3.9), we would like to use this feature by making a convolution between an exponential distribution (as in fig. 2.10) with varying μ and our data, in order to detect the heartbeat. In this step we assume that heartbeats are independent of each other and moreover the 'memorylessness' feature of the process. Peaks, and amplitude data, will be weighted according to the value of the distribution for a given μ, computing a new starting point (i.e., offset) which is centered on the point, is used as the position of the heartbeat. In order to decrease the computational effort, a time window is set to detect the following peak (i.e., $3s$),because it is quite reasonable to find the next heartbeat within 3 seconds after the previous one for a healthy individual. A few intermediate outputs of the algorithm are shown below (fig. 3.10).

Now, we run the algorithm taking into account of different possible means for the estimation of the heartbeat , as well as the different weights for the different contribution of convolution and filtered data. We thus obtain the result for duration of the heartbeat (fig. 3.11), which was first ordered according to the variance for estimation of a single heartbeat. This was due to the fact that we need an estimate as precise as possible. We can safely assume that the algorithm is more stable when the variance of the estimated parameter (duration of a single heartbeat) is low.

Our algorithm performs best for the convolution weight set at 100% and the mean of $0.63s$, Now, rerunning the algorithm for this value, in order to see pair-plots and infer something distinctive. At first we can say that there might be some dependence between the parameters used (weights and mean), and the results we obtain. For example: The convolution with the exponential distribution may be a strong assumption, since the value of the mean found for the duration of a heartbeat strongly depends on the value of μ which has been used as a parameter: the lower we have fixed it, the lower is the estimate that our algorithm returns.

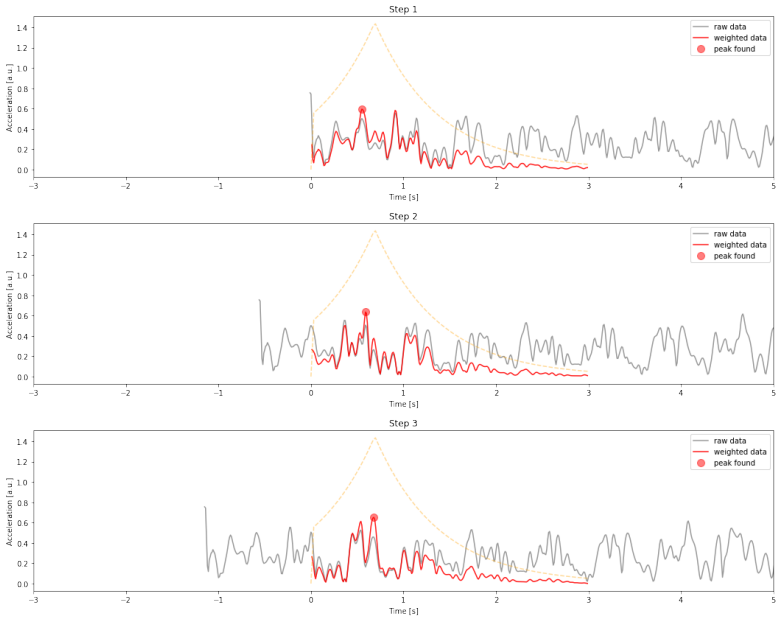

Figure 3.10: The figure represents the first 3 steps of the algorithm.

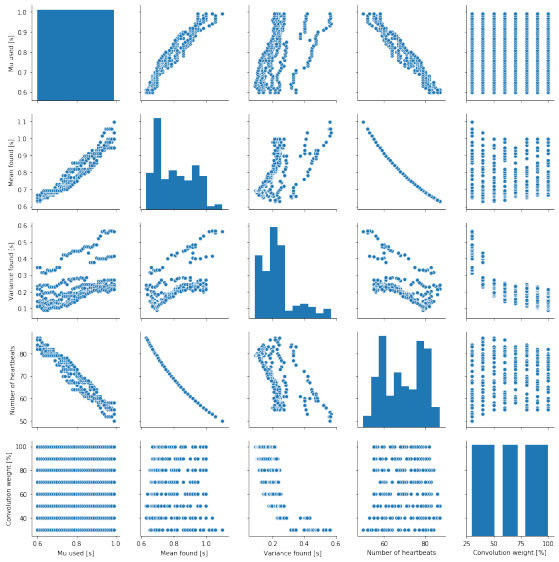

Figure 3.11: Results by running the algorithm for different values of the parameter μ for exponential distribution (from 0.60s to 1.00s), and convolution weights (from 10% to 100%, step of 10% each).

As we expected and stated above, there is a strong correlation not only between the mean we used for our algorithm, but also between the variance and the mean: the smaller is the mean used, the smaller are the mean returned and its variance. However, there is a region

Mu used [s]	Mean found [s]	Variance found [s]	Number of heartbeats	Convolution weight [%]
0.63	0.693671	0.087485	79	100.0
0.65	0.693671	0.090710	79	100.0
0.64	0.693671	0.091128	79	100.0
0.66	0.693671	0.099061	79	100.0
0.62	0.685000	0.099499	80	100.0
0.65	0.693671	0.099990	79	90.0
0.64	0.693671	0.100469	79	90.0
0.70	0.693671	0.104799	79	100.0
0.67	0.693671	0.104992	79	100.0
0.67	0.693671	0.105148	79	90.0

Figure 3.12: Table regarding first 10 lowest variance results.

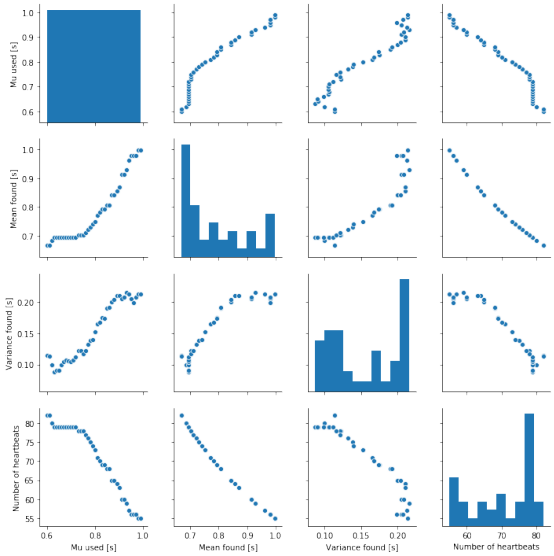

Figure 3.13: Results by running algorithm for the convolution weight parameter equal to 90%.

centered around 0.69s that is stable with respect to the change of the mean as a parameter.

Results given by the algorithm shown in table (fig. 3.12) are compatible with the previously obtained in figure (fig. 3.6 and we observe that the mean found are not that far from the mean obtained from the first technique, also the related variances are not large at all.

We thus conclude by stating that it is a good notion to use the exponential convolution, because the mean found resides in an interval which is really close to the estimate done in the first technique. Moreover our algorithm is stable in the stated region (i.e., μ used [0.60s, 0.72s]) (fig. 3.13. We shall need a larger data-set and some more parameters in order to make a cross reference and validate our results. The approximations and assumptions made seem correct at the first glance regarding mean obtained (fig. 3.14.

As previously done, we have also computed the HRV (Heart Rate Variability). In this case we notice that the points are distributed as a cluster, centered on the bisector line, but in a more sparse way when compared to the first data-set. In addition, taking a look into the timing distribution as a function of time we notice no pattern visible, moreover data as expected

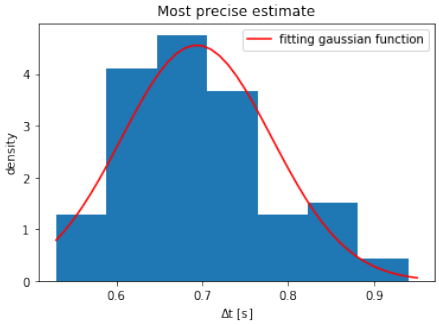

Figure 3.14: Histogram obtained by passing $\mu = 0.63s$ as parameter.

from HRV plot are sparser (fig. 3.15).

From these plots, we can not conclude whether our subject is healthy or not, since a larger data set is required.

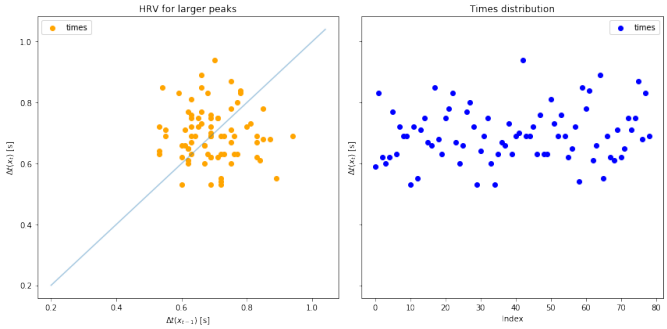

Figure 3.15: HRV computed by our algorithm ($\mu = 0.63s$).

4 RESULTS AND CONCLUSIONS

The results obtained in the analysis of the sensor placed on the sternum are the following:

- (70±5) BPM :for the accelerometer measurement in the Z axis (larger and smaller weighted peaks).
- (70±4) BPM :for the weighted gyroscope measurements in the two principal components.

As one can see the two results are excellently compatible. That means that both gyroscope and accelerometer can be used for the Heart rate evaluation. Since we have found two peaks in the accelerometer analysis for each heartbeat, we can extract more information about the duration of systolic and diastolic processes.

On the other hand for the sensor placed under the mattress the obtained results are:

- (90±15) BPM :for the accelerometer measurement in the Z axis (first technique)
- (87±11) BPM :for the accelerometer measurement in the Z axis (second technique)

Notice that the standard deviation is the largest in the last case, because of the noise introduced by the presence of the mattress.

This makes it is an uphill task to compare heartbeats between the two different data-sets because the data has been acquired at different moments of time and belongs to two different individuals.

The algorithms implemented are quite dissimilar from each other because of the different intrinsic nature of the data that belong to different populations.

This technique used is very robust, because it does not involve sophisticated electronics and physical contacts such as wires in the ECG. Exception is the sensor placed on the sternum.

The algorithm used is very simple. A person with the basics of programming can interpret and understand it easily.

The major drawback of this analysis is the availability of small data, from which the result obtained is not trustworthy. A large data-set analysis can reveal the ailments concerning to the heart in a better way.

REFERENCES

[1] B. Johansson, "A history of the electrocardiogram," *Dansk medicinhistorisk arbog*, pp. 163–176, 2001.

[2] J. Zanetti *et al.*, "Seismocardiography: A new technique for recording cardiac vibrations. concept, method, and initial observations," *Journal of cardiovascular technology (New York, NY)*, vol. 9, no. 2, pp. 111–118, 1990.

[3] I. Starr and F. C. Wood, "Twenty-year studies with the ballistocardiograph: the relation between the amplitude of the first record of" healthy" adults and eventual mortality and morbidity from heart disease," *Circulation*, vol. 23, no. 5, pp. 714–732, 1961.

[4] J. M. Zanetti and K. Tavakolian, "Seismocardiography: Past, present and future," in *2013 35th Annual International Conference of the IEEE Engineering in Medicine and Biology Society (EMBC)*, pp. 7004–7007, July 2013.